Acta Ophthalmologica

Acta Ophthalmologica 2022

Prediction of the axial lens position after cataract surgery using deep learning algorithms and multilinear regression

Achim Langenbucher,[1] Nóra Szentmáry,[2,3] Alan Cayless,[4] Jascha Wendelstein[5] and Peter Hoffmann[6]

[1]Department of Experimental Ophthalmology, Saarland University, Homburg/Saar, Germany
[2]Dr. Rolf M. Schwiete Center for Limbal Stem Cell and Aniridia Research, Saarland University, Homburg/Saar, Germany
[3]Department of Ophthalmology, Semmelweis-University, Budapest, Hungary
[4]School of Physical Sciences, The Open University, Milton Keynes, UK
[5]Department of Ophthalmology, Johannes Kepler University Linz, Linz, Austria
[6]Augen- und Laserklinik Castrop-Rauxel, Castrop-Rauxel, Germany

ABSTRACT.

Background: **The prediction of anatomical axial intraocular lens position (ALP) is one of the major challenges in cataract surgery. The purpose of this study was to develop and test prediction algorithms for ALP based on deep learning strategies.**

Methods: **We evaluated a large data set of 1345 biometric measurements from the IOLMaster 700 before and after cataract surgery. The target parameter was the intraocular lens (IOL) equator plane at half the distance between anterior and posterior apex. The relevant input parameters from preoperative biometry were extracted using a principal component analysis. A selection of neural network algorithms was tested using a 5-fold cross-validation procedure to avoid overfitting. The results were then compared with a traditional multilinear regression in terms of root mean squared prediction error (RMSE).**

Results: **Corneal radius of curvature, axial length, anterior chamber depth, corneal thickness, lens thickness and patient age were identified as effective predictive parameters, whereas pupil size, horizontal corneal diameter and Chang–Waring chord did not enhance the model. From the tested algorithms, the Gaussian prediction regression and the Support Vector Machine algorithms performed best (RMSE = 0.2805 and 0.2731 mm), outperforming the multilinear prediction model (0.3379 mm). The mean absolute prediction error yielded 0.1998, 0.1948 and 0.2415 mm for the respective models.**

Conclusion: **Modern prediction techniques may have the potential to outperform traditional multilinear regression techniques as they can deal easily with nonlinearities between input and output parameters. However, in all cases a cross-validation is mandatory to avoid overfitting and misinterpretation of the results.**

Key words: anatomical lens position – axial IOL position – deep learning – optical biometry – prediction model – regression model

Acta Ophthalmol. 2022: 100: e1378–e1384

doi: 10.1111/aos.15108

Background

Most of the classical IOL power calculation formulae such as Haigis (Haigis et al. 2000; Olsen 2007; Savini et al. 2020; Scholtz et al. 2021), Hoffer Q (Hoffer 1980; Hoffer 1993), Holladay1 (Holladay et al. 1988) or SRKT (Retzlaff et al. 1990) mainly differ—beside conversion of corneal radius of curvature to dioptric power with a keratometer index, offset values or limiters for input parameters—in different prediction models for the axial IOL position. This parameter is typically defined as the effective lens position (ELP), which does not necessarily coincide with the physical position of the IOL front surface (Olsen 2006), the IOL back surface or the image-side principal plane of the lens (Olsen & Hoffmann 2014).

The prediction of the axial position of an intraocular lens implant (IOL) in the eye after cataract surgery is one of the most relevant challenges in obtaining the target refraction. In a normal-sized eye, a prediction error of 100 micron in the axial lens position causes a prediction error in refraction of around 0.13 to 0.14 dpt. For example, when using the Javal Index ($n = 1.3375$) for the conversion of corneal radius of front curvature to dioptric power in the lens calculation formula, the focal length of the cornea is underestimated (or conversely, the

corneal power is overestimated). This has to be compensated with a larger dioptric power of the lens implant or alternatively with a slight displacement of the lens (Norrby & Koranyi 1997; Norrby 2004; Olsen & Hoffmann 2014) towards the retina (larger ELP).

Some modern lens power calculation concepts, such as the Olsen formula (Olsen 2007) or the Castrop formula (Langenbucher et al. 2021), tend towards calculating the real physical lens position (anatomical lens position (ALP), Norrby & Koranyi 1997; Norrby 2004) instead of the fictitious ELP (Olsen 2006; Olsen & Hoffmann 2014). For that task, the keratometer index for conversion of corneal front surface curvature to dioptric power is revised or updated to better describe the refracting properties of the cornea. In some concepts, correction terms for the axial length are used to consider the proportion of the eye media, especially in very long and short eyes (e.g. the Cooke correction). The ALP is mostly defined by the equatorial plane of the pseudophakic capsular bag with the implanted IOL with respect to the corneal corneal epithelium front apex. After cataract surgery, the ALP may be estimated from the pseudophakic anterior chamber depth and the central IOL thickness (Olsen 2006). This can be measured with good precision by modern optical biometers (Hirnschall et al. 2020). As a rough simplification, we can assume that the equatorial IOL plane is located at half the distance between the front and back vertex of the IOL. However, this could be affected by the shape factor or a step vault in the design. These are typically used to avoid rapid development of lens epithelial cell growth and posterior capsule opacification (Olsen 2006; Preußner et al. 2008; Scholtz et al. 2021). Modern lens power calculation concepts use the ALP value as a baseline and add slight (mostly constant) amounts of shift to consider the individual characteristics of IOL designs in terms of haptic and optic concept, refractive index and shape factor (Olsen 2007).

The most important benefit of the ALP compared with ELP concept is that the ALP can be directly validated after surgery using anterior segment tomographers or biometers, whereas the ELP as a fictitious value has to be calculated from the biometric parameters prior to cataract surgery, the power of the implanted IOL, and the achieved refraction after cataract surgery. This backtracing of the ELP (Melles et al. 2019; Savini et al. 2020) is routinely performed using a formula constant optimisation strategy, in which the biometric data, the power of the implanted lens and the refractive outcome of a sufficient number of clinical cases are used to determine post hoc the appropriate ELP and formula constant.

The purpose of this paper is to derive biometric measures of the eye prior to cataract surgery, using a large data set containing data from cataract surgeries from 1 clinical centre. The data recorded include corneal radius of curvature, axial length, central corneal thickness, anterior chamber depth, crystalline lens thickness, horizontal corneal diameter, Chang–Waring chord (as the difference between the coaxial light reflex and the pupil centre) in horizontal and vertical direction, and the patient's age and sex. These were used to develop both a classical regression-based prediction model and a neural network-based algorithm for predicting the axial position of the lens equator plane after cataract surgery.

Methods

Data set for the prediction model

A data set of 2231 measurements of a cataractous population before (at the timepoint of biometry for IOL power calculation) and 6 weeks to 3 months after cataract surgery with the biometer (IOLMaster 700, Carl-Zeiss Meditec, Jena, Germany) was evaluated in this study. Three hydrophobic monofocal aspherical lenses were considered: Clareon, Alcon, Fort Worth, USA; Vivinex, Hoya Surgical, Tokyo, Japan; and ZCB00, Johnson & Johnson, New Brunswick, USA). These 3 lenses do not differ significantly in the general optical design or in the optimized formula constants (Clareon119.1; ZCB00: 119.4; Vivinex: 119.2, data derived from https://IOLCon.org at 12th October 2021).

All data were obtained from one clinical centre (2 experienced surgeons, Augen- und Laserklinik, Castrop-Rauxel, Germany). This study was registered at the local Ethics Committee (Ethikkommission der Ärztekammer des Saarlandes with the registration number 157/21). The data were anonymised by the source and transferred to a .csv data table using the software module for batch data export. The data tables were reduced to the relevant parameters required for our data analysis, consisting of the following measurements extracted from the preoperative measurement: the patient's age (Age) in years as the time interval from date of birth to the preoperative measurement, the laterality (left or right eye), sex (female or male), flat (R1) and steep (R2) corneal radius of curvature both in mm, axial length (AL) in mm, central corneal thickness (CCT) in mm, anterior chamber depth (ACD) in mm (measured from corneal epithelium to lens), central thickness of the crystalline lens (LT) in mm, pupil diameter (PD), horizontal corneal diameter (CD) in mm, plus the Chang–Waring chord as the distance between the light reflex originating from a coaxial light source (Purkinje reflex P I) and the pupil centre (Chang & Waring GO 4th 2014, distance CWchord in mm and axis CWchordA in °). From the postoperative measurement, we extracted the pseudophakic anterior chamber depth (ACD_{po}) in mm and the central IOL thickness (LT_{po}) in mm. Only one eye from each subject was included in this study. Where measurements of both eyes were available, one eye was randomly selected. Subjects with missing data or data with a 'Failed' or 'Warning' in the internal quality check of the IOLMaster 700 for R1, R2, AL, CCT, ACD, LT, PD, CD, CWchord, CWchordA, ACD_{po} or LT_{po} were excluded. After checking for 'Successful' measurement for corneal front and back surface curvature data, a data set of $N = 1345$ measurements was used for training, validation and test of our prediction algorithm. The data were transferred to Matlab (Matlab Version 2019b, MathWorks, Natick, USA) for further processing.

Data preprocessing in Matlab

From the corneal curvature in the flat and steep meridian, we derived the mean corneal curvature R in mm as $R = 0.5 \cdot (R1 + R2)$. The Chang–Waring chord as given by the IOLMaster 700 in distance and direction was converted to vector components in the horizontal ($CWX = CWchord \cdot \cos(CWchordA)$) and vertical (CWY =

CWchord·sin(CWchordA)) axes, both in mm. In addition, to consider the laterality, the horizontal component of CWX was flipped in sign for left eyes CWX_{cor} to get negative values for a temporal shift and positive values for a nasal shift. The equator plane of the IOL (LEQ) in mm as target parameter in our study was assumed to be located at half the distance between the IOL front and back apex ($LEQ = ACD_{po} + 0.5 \cdot LT_{po}$). The difference between LEQ derived from the measured ACD_{po} and LT_{po} and the LEQ predicted by our model (LEQ_{pred}) was considered as the prediction error ($LEQ - LEQ_{pred}$).

Modelling in Matlab

In a first step, a feature selection in terms of a principal component analysis (PCA) was used to identify the relevant input parameters for our prediction models (Herrmann 1997). PCA is a commonly used strategy to decompose the parameters in the parameter space into an orthonormal basis in order to extract the most relevant input parameters for dimensionality reduction in explorative data analysis and prediction models (Kleesiek et al. 2020). The order of principal components within the parameter space is chosen to maximize the variance of the data set. In our setup, we defined a benchmark of 99% of the variance in the data to be preserved with the PCA and dimensionality reduction.

In a second (qualification) step, a selection of classical neural network types (Bechtel 2008; Welsch et al. 2018; Sramka et al. 2019; Carmona González & Palomino Bautista 2021; Langenbucher et al. 2020) was tested on the data set to determine the performance in terms of predicting the LEQ from the relevant input parameters identified by the PCA. The following neural network algorithms were tested:

- Regression models: 4 different options were implemented with simple multilinear regression, multilinear regression with interactions between input parameters, a robust setup with individual weighting of the data points and a stepwise linear fitting by including and excluding components.
- Regression trees: 3 different options were implemented. A tree with a high resolution (fine tree) and plenty of leaves with a minimum leaf size of 4, a tree with a normal resolution (normal tree) and an average leaf size of at least 12, and a tree with a coarse resolution (coarse tree) with a restriction to some large leaves with a minimum leaf size of 36.
- Support vector machines (SVM): 4 different options were implemented. SVM were considered with a linear kernel, with a quadratic kernel, a cubic kernel and a Gaussian kernel. The preset kernel size was selected as ¼ of the square root of the number of effective predictive parameters.
- Gaussian process regression (GPR): 3 different options were tested in our setup: with a GPR with a squared exponential function for the kernel, with an exponential function for the kernel, and a GPR with a rational quadratic kernel, which allows a flexible model fit with variation to different scales.To evaluate the performance of each algorithm under test, we extracted the root mean squared prediction error (Welsch et al. 2018).

To avoid overfitting of the models, the entire data set of $N = 1345$ measurements was split randomly into 5 equally sized clusters ($N = 269$ each), and with a 5-fold cross-validation strategy, the neural network algorithms were trained with the training set ($N = 1076$, excluding the test set) and validated with the test set ($N = 269$), with permutations until each cluster was excluded once (Bechtel 2008).

In a third step, the 2 most promising neural network approaches from the tested neural network types in terms of smallest root mean squared prediction error were analysed more in detail. For reference, we defined a classical multilinear regression model having the same input parameters, predicting LEQ as the output parameter. To ensure a fair comparison, we implemented a cross-validation strategy for the multilinear regression model using the data partitions defined for the neural network approaches.

Statistics

The input parameters and the target parameter are shown in Table 1 with mean, standard deviation, median and 90% confidence interval (5% and 95% quantile). For the 3 prediction models (the 2 neural network approaches with the least root mean squared prediction error and the classical multilinear regression model), we provide the mean prediction error (ME) with standard deviation (SD), the mean absolute prediction error (MAE), the 95% quantile (CL90) of the absolute prediction error (as the absolute prediction error shows in general a one-sided distribution) and the root mean squared prediction error (RMSE). For the multivariate linear prediction model, we used maximum likelihood estimation with iterative ECM algorithm (Meng et al. 1993; Sexton & Swensen 2000), and the respective results are described with the coefficient of determination (CoD), Sigma and LogL as the value of the log likelihood objective function after the final iteration.

Results

We included $N = 1345$ measurements from 669 left eyes in this study (787 eyes from female patients). Table 1 shows a listing of the mean value, standard deviation, median, minimum and maximum, as well as the 90% confidence intervals of biometric al input and target parameters used for our modelling. The CW chord shows a trend towards the inferior direction and a horizontal shift in the temporal direction (which can be seen from the data of CWX_{cor}, but not from CWX).

In a first step, the feature selection in terms of a PCA was applied to identify the most relevant input parameters: age, R, AL, CCT, ACD and LT were included in the prediction models as input parameters (or effective predictive parameters), whereas the sex, PD, CD, CWX and CWY were identified as parameters, which did not significantly improve the model performance.

In the second step of testing, the performance of prediction models using a selection of neural network strategies we determined that the family of regression networks yielded a RMSE in a range between 0.32123 mm (linear regression with interactions between parameters) and 0.32801 mm (robust linear regression). With the family of regression trees, the RMSE ranged between 0.33442 mm (coarse tree) and 0.34588 mm (fine tree). With the family of support vector machines, we obtained a RMSE in the range of 0.28052 mm(SVM with a quadratic

Table 1. Explorative data of the input parameters and the target parameter for our prediction model in terms of mean value, standard deviation, median and 90% confidence interval.

N = 1345	Age in years	R in mm	ACD in mm	LT in mm	CCT in mm	CD in mm	PD in mm	CWX in mm	CWX_{cor} in mm	CWY in mm	LEQ in mm	
	Mean	70.63	7.73	3.13	4.63	0.56	12.00	4.15	−0.03	−0.26	−0.11	5.14
	Standard deviation	9.72	0.28	0.42	0.46	0.04	0.42	1.23	0.34	0.22	0.20	0.43
	Median	72.22	7.71	3.17	4.61	0.56	11.99	3.90	−0.03	−0.26	−0.11	5.12
	5% quantile	52.57	7.30	2.42	3.88	0.50	11.36	2.54	−0.55	−0.60	−0.39	4.46
	95% quantile	83.85	8.23	3.77	5.41	0.62	12.68	6.81	0.50	0.04	0.16	5.86

Age refers to the patient age at the timepoint of the biometric measurement before cataract surgery, R to the average corneal curvature (mean value of corneal curvature in the flat and steep meridian), ACD to the phakic anterior chamber depth as the distance between the front corneal apex and the front lens apex, LT to the central thickness of the crystalline lens, CCT to the central corneal thickness, CD to the horizontal corneal diameter, PD to the pupil diameter, CWX and CWY to the horizontal and vertical component of the CW chord, CWX_{cor} to the CWX where the sign was flipped for left eyes, and LEQ to the axial position of the equator plane of the intraocular lens considered as half the distance between the anterior and posterior apex of the intraocular lens.

kernel) and 0.29421 mm (SVM with a Gaussian kernel architecture), and for the family of GPR algorithms, we derived a range for RMSE between 0.27304 mm (GPR with exponential kernel) and 0.29086 mm (GPR with rational quadratic kernel). The 2 neural network algorithms with the best performance in terms of least root mean squared prediction error were the GPR with exponential kernel (RMSE = 0.27034 mm) and the SVM with a quadratic kernel (RMSE = 0.28052 mm), and these were analysed in more detail. The robust multilinear prediction model with the input parameters age, R, AL, CCT, ACD and LT with 5-fold cross-validation showed a performance of RMSE = 0.33794 mm (LogL = −593.5, Sigma = 0.1079, CoD = 0.386). The overall multilinear regression model is characterized with the regression coefficients (from *N* = 1345 measurements) as follows:

$$LEQ_{pred} = 1.1065 - 0.0003 \cdot Age - 0.0935 \cdot R + 0.0382 \cdot AL - 0.0430 \cdot CCT + 0.7070 \cdot ACD + 0.3614 \cdot LT.$$

Table 2 shows the explorative performance data of both neural network algorithms and the multilinear regression model in terms of mean and standard deviation of the prediction error; the median prediction error, mean absolute and root mean squared prediction error, and the upper limit of the 90% and 99% confidence interval of the absolute prediction error.

The GPR algorithm that proved to have the lowest root mean squared prediction error on our data set showed a MAE/RMSE, which was 19.3%/19.2% lower compared with the respective prediction error of the multilinear regression model. Figure 1 displays the performance plot with the predicted LEQ *versus* the LEQ derived from the postoperative anterior chamber depth and lens thickness for the GPR algorithm with exponential kernel, the SVM with quadratic kernel (Bechtel 2008) and the multilinear prediction model all with a 5-fold cross-validation. Data points on the diagonal (as indicated by the red line) show no prediction error.

Both neural network approaches show a slightly flatter trend, meaning that large values of LEQ are underestimated and small values overestimated. In contrast, the multilinear regression algorithm systematically underestimates large LEQ values and overestimates small LEQ values, with a larger data scatter.

Table 2. Descriptive performance data of the 2 neural network approaches with the least root mean squared prediction error out of the selection of algorithms under test. All data were derived with a 5-fold cross-validation strategy to avoid overfitting.

N = 1345	GPR with exponential kernel	SVM with quadratic kernel	Multilinear regression model	
	Mean prediction error ME in mm	0.0007	−0.0260	−0.0001
	SD of prediction error in mm	0.2732	0.2794	0.3380
	Median prediction error in mm	0.0228	−0.0101	−0.0358
	Mean absolute prediction error MAE in mm	0.1948	0.1998	0.2415
	Root mean squared prediction error RMSE in mm	0.2731	0.2805	0.3379
	95% quantile of absolute prediction error in mm	0.5390	0.5698	0.6902
	99.5% quantile of absolute prediction error in mm	0.9675	0.9524	1.1496

GPR = Gaussian process regression neural network; SD = standard deviation; SVM = support vector machine.
For the multilinear regression model, we used a robust ECM algorithm.

Discussion

The prediction of the axial IOL position with preoperative biometric data is one of the largest challenges in intraocular lens power calculation (Norrby & Koranyi 1997; Melles et al. 2019). Many competing concepts for estimating the lens position have been proposed. The simplest versions are based on K readings derived from corneal front surface curvature and axial length, or on several other parameters such as phakic anterior chamber depth, lens thickness, horizontal corneal diameter or patient age. However, we also have to take into consideration that most of the lens power calculation concepts involve estimation of an ELP, which does not match the anatomical position of the IOL in the

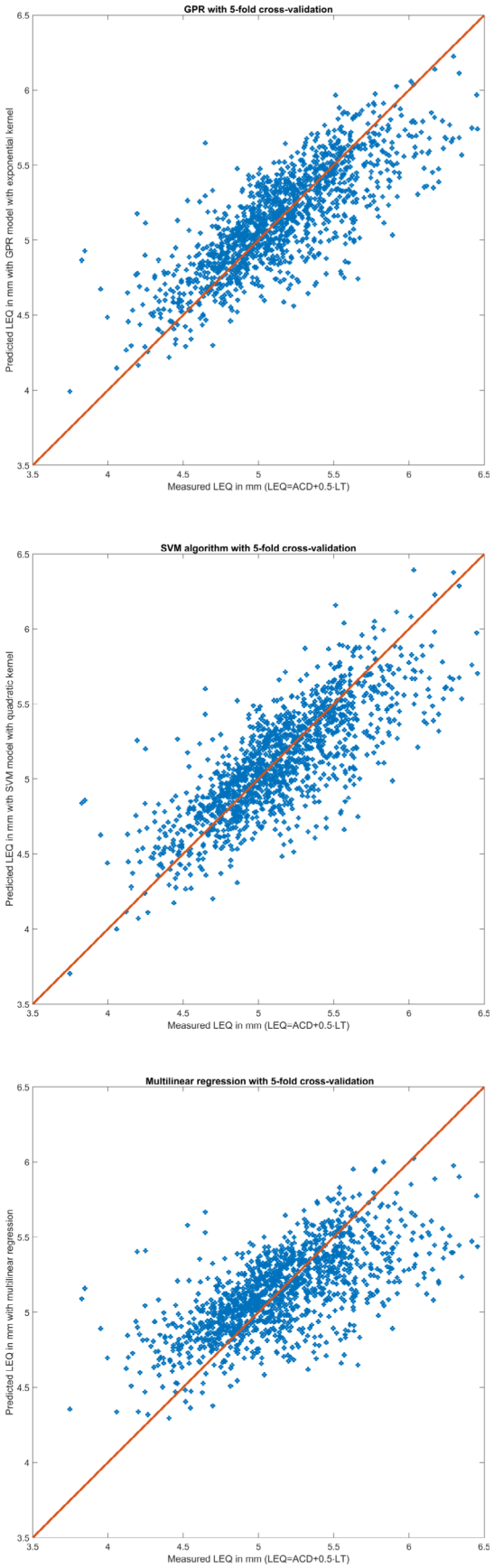

Fig. 1. Performance plot of the 2 neural network approaches with the lowest root mean squared prediction error on our data set (Gaussian prediction regression (GPR) with an exponential kernel, upper graph; Support Vector Machine (SVM) algorithm with a quadratic kernel, middle graph) and the respective performance plot for the multilinear regression model (lower graph, also with 5-fold cross-validation) together with the red diagonal line indicating data where the predicted LEQ matches the LEQ derived from measured ACD and LT after surgery. Both neural network approaches show a trend, which is slightly flatter compared with the red line. This implies that large LEQ values are slightly underestimated and small LEQ values are slightly overestimated. In contrast, the multilinear regression shows a significantly flatter trend with a underestimation/overestimation of large/small LEQ values and a larger scatter compared with the neural network approaches.

eye (Olsen & Hoffmann 2014; Scholtz et al. 2021). The ELP is back-calculated from the preoperative biometric data, the power of the inserted lens and the postoperative refraction, and typically covers all systematic errors of biometry, lens power-labelling errors or errors in refractometry (e.g. offset errors due to the measurement lane distance). Some modern formulae such as the Olsen (Olsen 2007) or the Castrop formula (Langenbucher et al. 2021) made a paradigm change in considering the 'true' axial lens position, either as the front apex plane or the equator plane of the lens, instead of the ELP. However, even with this 'anatomical lens position' (ALP), we cannot solve all problems in IOL power calculation as, while according to ISO 11979 standards, the equivalent power is labelled on the lens, the respective image-sided principal plane is still unknown because the shape of the lens is not provided by the IOL manufacturer. However, using a reliable concept for ALP (Norrby 2004) prediction, valid for all lens types and considering the lens optics and haptics characteristics such as the refractive index, the haptics shape and angulation, (and the shape factor step vault of the lens design) with a constant or individual offset to the ALP, might be a significant step towards better prediction of the refractive outcome

(Olsen 2006; Xin et al. 2020). As the design data of IOLs on the market are currently unavailable, we decided to use a simple estimate for the IOL equator plane, defining this as half the distance between the lens front and back apex. This definition might be refined if data on the lens shape become available in the future.

The simplest way of predicting the ALP is based on a multilinear modelling, provided a data set with preoperative biometric data and the postoperative measurement of the axial lens position is available. In this case, the ALP is derived from a sum of intercept and weighted input parameters. Modern optical biometers are capable of measuring all the distances in the eye, not only for the phakic eye prior to cataract surgery, but also in the pseudophakic eye after cataract surgery (Cheng et al. 2020). If we have derived the IOL position—either the IOL front apex or an estimate for the lens equator as in this study—the relevant predictive parameters to keep the model simple and to avoid overfitting must be identified (Bechtel 2008; Welsch et al. 2018). In the present study, the predictive parameters were analysed using a feature selection strategy based on a principal component analysis. Alternatively, a stepwise iterative fit strategy was used, initialized as a constant model adding and subsequently removing potential parameters in a stepwise fashion to refine the model while explaining as much variance in the data set as possible. Subsequently, a multilinear model is set up with the relevant predictive parameters, either in a simple version by minimizing the root mean squared prediction error or in a more sophisticated version with some robustness constraints as was performed here with the ECM algorithm (Meng et al. 1993; Sexton & Swensen 2000).

In the last decade, traditional techniques such as (multi-)linear models have increasingly competed with modern machine learning strategies, as they can easily adapt to nonlinear behaviour of the target parameter with respect to the input parameters, whereas linear regression models mostly fail (Clarke & Burmeister 1997; Sramka et al. 2019; Carmona González & Palomino Bautista 2021; Langenbucher et al. 2020; Xia et al. 2020). The most complex aspect of implementing such deep learning techniques is in identifying the most reliable prediction algorithm from a large number of available algorithms. It is also necessary to avoid overfitting, which may result either from considering too many input parameters or from evaluating the performance of the algorithm using the same data set, which was used for training. In the present study, to avoid overfitting, we performed our PCA to extract the relevant input parameters and then implemented a cross-validation procedure involving a strict separation of training and test data during the validation process. To make cross-validation efficient, a 5-fold cross-validation was used. In this strategy, the data set is split into 5 partitions, and one partition excluded during training, to be used for testing later on. This procedure is repeated until all partitions have been used for validation. Where very large data sets are available, simpler strategies such as holdout or random subsampling could be applied as an alternative to cross-validation. The effect of ignoring cross-validation is shown for the multilinear prediction model on the performance plot in Fig. 2.

In generating this plot, we used the same multilinear fit algorithm with iterative ECM as was used to generate the lowest graph in Fig. 1, but without splitting the data into partitions for training and validation. The respective prediction error if all $N = 1345$ measurements are used for training and validation yields: mean prediction error 0.0000 mm, standard deviation 0.3158 mm, median prediction error −0.0355 mm, mean absolute prediction error 0.2258 mm, root mean squared prediction error of 0.3157 and the upper limits of the 90% and 99% confidence intervals of the absolute prediction error 0.6437 and 1.0824 mm.

In the present study, we evaluated several versions of regression networks,

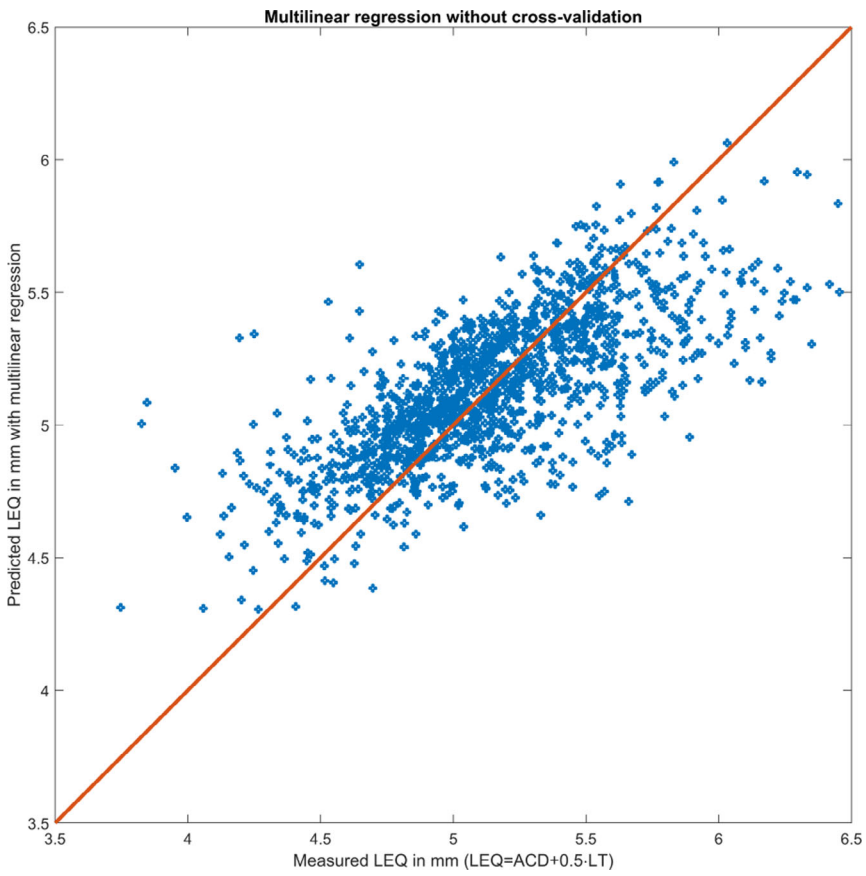

Fig. 2. Performance plot of the multilinear regression model without cross-validation. The entire data set of $N = 1345$ measurements was used both for training and validation. The performance of the model is significantly better compared to the respective performance with 5-fold cross-validation (compare Fig. 1 lowest graph) indicated by a lower scatter of the data. The red line indicates data where the predicted LEQ matches the LEQ derived from measured ACD and LT after surgery.

regression trees, Support Vector Machines and Gaussian process regression networks, as they are very popular (Welsch et al. 2018). The root mean squared prediction error was used as a target criterion for evaluating the performance of the algorithm and for ranking. Ultimately, we identified the Gaussian process regression network with and exponential kernel and the Support Vector Machine network with a quadratic kernel as the algorithms with the best performance. However, such a selection cannot be generalized to other applications as it mostly depends on the data set and on the performance criterion. The GPR algorithm outperformed the multilinear regression by around 19% (MAE) to 20% (RMSE). This does not, however, mean that the prediction error of lens power calculation could be reduced by the same amount, as the estimation of the axial IOL position is only one (albeit very important) determinant for predicting the refractive outcome after cataract surgery (Olsen 2006). Nevertheless, we feel that for IOL power calculation strategies, which use ALP instead of ELP, this might be a step towards better predictability of the refractive outcome. However, the advantages of such deep learning strategies for prediction of ALP have to be carefully validated with clinical studies.

In conclusion, in the present paper, we have attempted to develop and implement a strategy for predicting the position of the lens equator plane after cataract surgery derived from postoperative biometric measurements from biometric measurements before cataract surgery, which is routinely performed for lens power calculation. Modern techniques of machine learning algorithms were compared with the respective results of a traditional multilinear regression, and it seems that lens position prediction could significantly benefit from these deep learning strategies in the future.

References

Bechtel S (2008): Maschinelles Lernen in der Medizin – Anwendung von Support Vector Machines in der Ganganalyse. Diplomarbeit Fachbereich Mathematik, Universität des Saarlandes.

Carmona González D & Palomino Bautista C (2021): Accuracy of a new intraocular lens power calculation method based on artificial intelligence. Eye (Lond) **35**: 517–522. Epub 2020 Apr 28. doi: https://doi.org/10.1038/s41433-020-0883-3

Chang DH & Waring GO 4th (2014): The subject-fixated coaxially sighted corneal light reflex: a clinical marker for centration of refractive treatments and devices. Am J Ophthalmol **158**: 863–874.

Cheng H, Kane JX, Liu L, Li J, Cheng B & Wu M (2020): Refractive predictability using the IOLMaster 700 and artificial intelligence-based IOL power formulas compared to standard formulas. J Refract Surg **36**: 466–472.

Clarke GP & Burmeister J (1997): Comparison of intraocular lens computations using a neural network versus the Holladay formula. J Cataract Refract Surg **23**: 1585–1589.

Haigis W, Lege B, Miller N & Schneider B (2000): Comparison of immersion ultrasound biometry and partial coherence interferometry for intraocular lens calculation according to Haigis. Graefes Arch Clin Exp Ophthalmol **238**: 765–773.

Herrmann J (1997): Maschinelles lernen und wissensbasierte systeme. Heidelberg: Springer.

Hirnschall N, Findl O, Bayer N, Leisser C, Norrby S, Zimper E & Hoffmann P (2020): Sources of error in toric Intraocular lens power calculation. J Refract Surg **36**: 646–652.

Hoffer KJ (1980): Steps for IOL power calculation. Am Intraocul Implant Soc **6**: 370.

Hoffer KJ (1993): The Hoffer Q formula: a comparison of theoretic and regression formulas. J Cataract Refract Surg **19**: 700–712. Erratum: J Cataract Refract Surg 1994; 20: 677. Letter to the Editor: Eye (2007) 21, 429. doi:; published online 29 September 2006

Holladay JT, Prager TC, Chandler TY, Musgrove KH, Lewis JW & Ruiz RS (1988): A three-part system for refining intraocular lens power calculations. J Cataract Refract Surg **14**: 17–24.

Kleesiek J, Murray JM, Kaissis G & Braren R (2020): Künstliche Intelligenz und maschinelles Lernen in der onkologischen Bildgebung. Onkologe **26**: 60–65.

Langenbucher A, Szentmáry N, Cayless A, Weisensee J, Fabian E, Wendelstein J & Hoffmann P (2021): Considerations on the Castrop formula for calculation of intraocular lens power. PLoS ONE **16**: e0252102.

Langenbucher A, Szentmáry N, Wendelstein J & Hoffmann P (2020): Artificial intelligence, machine learning and calculation of intraocular lens power. Klin Monatsbl Augenheilkd **237**: 1430–1437.

Melles RB, Kane JX, Olsen T & Chang WJ (2019): Update on intraocular lens calculation formulae. Ophthalmology **126**: 1334–1335.

Meng XL, Xiao L & Rubin DB (1993): Maximum likelihood estimation via the ECM algorithm. Biometrika **80**: 267–278.

Norrby NE & Koranyi G (1997): Prediction of intraocular lens power using the lens haptic plane concept. J Cataract Refract Surg **23**: 254–259.

Norrby S (2004): Using the lens haptic plane concept and thick-lens ray tracing to calculate intraocular lens power. J Cataract Refract Surg **30**: 1000–1005.

Olsen T & Hoffmann P (2014): C constant: new concept for ray tracing-assisted intraocular lens power calculation. J Cataract Refract Surg **40**: 764–773.

Olsen T (2007): Calculation of intraocular lens power: a review. Acta Ophthalmol Scand **85**: 472–485.

Olsen T (2006): J Prediction of the effective postoperative (intraocular lens) anterior chamber depth. J Cataract Refract Surg **32**: 419–424.

Preußner PR, Olsen T, Hoffmann PC & Findl O (2008): Intraocular lens calculation accuracy limits in normal eyes. J Cataract Refract Surg **34**: 802–808.

Retzlaff JA, Sanders DR & Kraff MC (1990): Development of the SRK/T intraocular lens implant power calculation formula. J Cataract Refract Surg **16**: 333–340.

Savini G, Taroni L & Hoffer KJ (2020): Recent developments in intraocular lens power calculation methods-update 2020. Ann Transl Med **8**: 1553.

Scholtz S, Cayless A & Langenbucher A (2021): Calculating the human eye—basics on biometry. In: Liu C & Bardan AS (eds). Cataract surgery. Cham: Springer. https://doi.org/10.1007/978-3-030-38234-6_7

Sexton J & Swensen AR (2000): ECM algorithms that converge at the rate of EM. Biometrika **87**: 651–662.

Sramka M, Slovak M, Tuckova J & Stodulka P (2019): Improving clinical refractive results of cataract surgery by machine learning. PeerJ **7**: e7202.

Welsch A, Eitle V & Buxmann P (2018): Maschinelles Lernen. HMD **55**: 366–382.

Xia T, Martinez CE & Tsai LM (2020): Update on intraocular lens formulas and calculations. Asia Pac J Ophthalmol **9**: 186–193.

Xin C, Bian GB, Zhang H, Liu W & Dong Z (2020): Optical coherence tomography-based deep learning algorithm for quantification of the location of the intraocular lens. Ann Transl Med **8**: 872.

Received on October 22nd, 2021.
Accepted on January 20th, 2022.

Correspondence:
Achim Langenbucher
Department of Experimental Ophthalmology
Saarland University
Kirrberger Str 100 Bldg. 22.
66424 Homburg
Germany
Tel: +49 6841 1621218
Fax: +49 6841 1621240
Email: achim.langenbucher@uks.eu

Open Access funding enabled and organized by Projekt DEAL.